The Vector Fitting Approach to Simulation of EM Fields Radiated by UWB Sources Placed on Convex Conducting Surface

Piotr Gorniak, Wojciech Bandurski
Poznan University of Technology
Poznan, Poland
pgorniak@et.put.poznan.pl

Abstract— **The paper presents a new approach to time-domain effective calculation of electromagnetic fields radiated by an UWB sources placed on conducting convex obstacle. The frequency domain uniform theory of diffraction (UTD) and rational approximation exploiting the vector fitting algorithm (VF) is used for deriving the closed form time domain function of the radiated field. The VF algorithm is performed with respect to new generalized variables proportional to frequency but also taking into account geometrical parameters of the obstacle. The Spice simulation is used for calculation of numerical examples.**

Index Terms— **ultra-wideband, vector fitting, universal Fock radiation functions, conducting cylinder.**

I. Introduction

Ultra-wideband (UWB) technology enables many beneficial possibilities in telecommunication area [1]. In order to take advantage of these possibilities, careful analysis of a given UWB system is required, in particular analysis of the propagation channel.

In this paper we focus our considerations on effective time domain modeling of radiation of electromagnetic (EM) wave by UWB sources placed on convex conducting cylinders which in practice can be used as models of real convex objects (e.g. people [2]). Our aim is to present the method for obtaining a simple, closed form impulse response dedicated for the described UWB radiation scenario. We use the Uniform Theory of Diffraction (UTD) in our analysis. For the sake of clarity and simplicity of the description of our approach we consider the TE polarisation case only (taking into account z-directed magnetic current source), Fig. 1. In the paper we give a simple, closed form impulse response of a ray associated with such radiation scenario, as well as the procedure for obtaining it.

The analytical description of the radiation of EM wave by sources placed on convex surface in the time and the frequency domain was already considered in the literature, e.g. [3, 4]. The disadvantage of these solutions can be a long time of computations associated with them.

In this paper, we introduce a universal rational approximation, valid for cases of direct rays as well as creeping rays and independent of geometry of the radiation scenario, and of the frequency band. For this purpose, we introduce new variables for which we carry out universal rational function approximations by means of the VF algorithm [5]. These new variables depend on the frequency and the geometry of a radiation scenario. Using this approach we have to perform the rational approximation once. The obtained coefficients can be then used in many other scenarios and frequency ranges. In this way we obtain a universal approximation of the transfer function for the ray associated with a radiation scenario (radiation ray) that can be used for all considered scenario geometries and frequency bands (of course in reasonable limits).

The rest of the paper is organized as follows. In Section II we revise the concept of the UTD transfer function for a radiation ray. In section III we describe the procedure of obtaining the closed form universal rational approximation of the transfer function of a radiation ray. Simulation of the UWB radiation in a SPICE simulator is shown in Section IV. In section V some examples are given. Section VI concludes the paper.

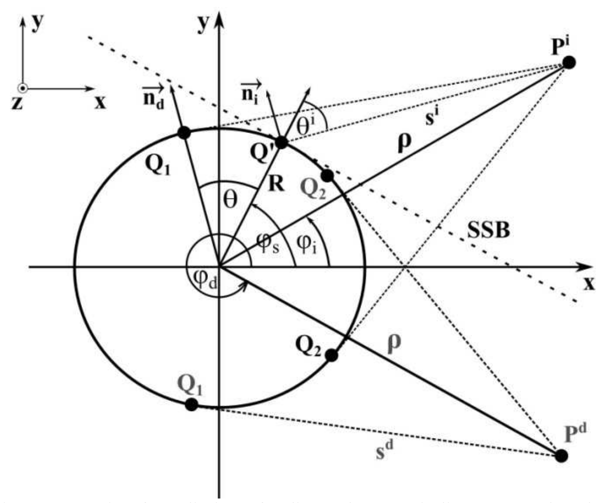

Fig. 1. Scenario of a radiation of z-directed magnetic line source placed at the point Q'on conducting 2D cylinder. SSB is the Surface Shadow Boundary.

II. THE UTD RADIATION RAY UNIVERSAL TRANSFER FUNCTION

The scenario of direct and creeping radiation rays for observation points placed in the lit as well as shadow zones for the case of 2D conducting cylinder is shown in Fig. 1. The observation point in the lit and the shadow zones are marked with P^i and P^d, respectively. The position of z-directed magnetic current source is at Q'. The counterclockwise and clockwise shedding points are marked with Q_1 and Q_2, respectively. The main parameters of the scenario are: R – the radius of cylinder, θ – the radial length of distances along which propagates a creeping ray from point Q' to the shedding point. The distances along which the EM wave propagates in the air are denoted by s^i and s^d for direct and creeping ray, respectively. The electric field vectors associated with a radiation ray at the observation point are directed along the unit vectors $\overrightarrow{\boldsymbol{n_i}}$ or $\overrightarrow{\boldsymbol{n_d}}$ for the case of direct or creeping ray respectively.

Fourier transforms of the time-domain derivative of TE polarized magnetic current source – M(ω) and the electric filed at the observation point – $E^P(\omega)$ for one radiation ray (Fig.1) are related by the expression [3]:

$$E^P(\omega)=M(\omega)H_{rad}(\omega)A_c\left(s^{i/d}\right)\exp\left(-j\omega s_p/v_0\right) \qquad (1)$$

where s_p is the total length of the radiation ray, v_0 is the speed of EM wave in free space, $A_c(s^{i/d})$ is equal to $(s^i)^{-0.5}$ and $(s^d)^{-0.5}$ for the case of direct and creeping ray, respectively [6] and $H_{rad}(\omega)$ is the part of the transfer function of a radiation ray that will be approximated with VF algorithm.

The transfer function $H_{rad}(\omega)$ is defined with universal Fock radiation functions [3, 6]. For TE polarized magnetic current source case $H_{rad}(\omega)$ is given by [6]:

$$H_{rad}(\omega)=-\exp(-j\pi/4)\sqrt{\frac{\omega}{8\pi\cdot v_0}}G\left(\xi^{i/d}\right) \qquad (2)$$

where G(x) is the universal Fock radiation function for TE polarisation case, variable $\xi^{i/d}$ is defined by (3a) and (3b) for the case of direct and creeping ray, respectively, (Fig. 1) and the associated curvature parameter is given by (4):

$$\xi^{i/d}=\xi^i=-m\cdot\cos\left(\theta^i\right) \qquad (3a)$$

$$\xi^{i/d}=\xi^d=m\cdot\theta \qquad (3b)$$

$$m=\left(\frac{\omega\cdot R}{2v_0}\right)^{1/3} \qquad (4)$$

In order to find the universal VF approximation of (2) dedicated to general, practical UWB scenarios, we rearrange $H_{rad}(\omega)$ into a function of new variables, ξ^i_{sub} and ξ^d_{sub} for direct and creeping ray case, respectively. The new variables are given by:

$$\xi^i_{sub}=-\frac{\omega R}{2v_0}\cos^3\left(\theta^i\right) \qquad (5a)$$

$$\xi^d_{sub}=-\frac{\omega R}{2v_0}\theta^3 \qquad (5b)$$

Now transfer function (2) for the case of direct and creeping ray obtain the form given by (6a) and (6b), respectively:

$$\begin{aligned}H_{rad}(\omega)=H^i_{rad}(\omega)=-\sqrt{\frac{1}{4\pi R\cdot\cos^3\left(\theta^i\right)}}\exp(j\pi/4)\times\\ \sqrt{-\xi^i_{sub}}G\left(\xi^{i\ \ 1/3}_{sub}\right)=\sqrt{\frac{1}{4\pi R\cdot\cos^3\left(\theta^i\right)}}\cdot V^i\left(\xi^i_{sub}\right)\end{aligned} \qquad (6a)$$

$$\begin{aligned}H_{rad}(\omega)=H^d_{rad}(\omega)=-\sqrt{\frac{-j}{4\pi R\cdot\theta^3}}\exp(j\pi/4)\times\\ \sqrt{\xi^d_{sub}}G\left(\xi^{d\ \ 1/3}_{sub}\right)=\sqrt{\frac{1}{4\pi R\cdot\theta^3}}\cdot V^d\left(\xi^d_{sub}\right)\end{aligned} \qquad (6b)$$

The analogous formulas to the two above equations for the case of TM polarized magnetic current source as well as the case of electric current source are not given in the paper but can be found easily using the theory given in e.g. [6]. In order to find the universal simple in form time domain equivalents of (6a) and (6b) functions $V^i\left(\xi^i_{sub}\right)$ and $V^d\left(\xi^d_{sub}\right)$ will be approximated with VF algorithm in the predefined domain limits.

III. VF APPROXIMATION

In order to apply VF approximation for $\boldsymbol{V^i\left(\xi^i_{sub}\right)}$ and $\boldsymbol{V^d\left(\xi^d_{sub}\right)}$ we determine the ranges of variables $\boldsymbol{\xi^i_{sub}}$ and $\boldsymbol{\xi^d_{sub}}$. These ranges should reflect the values of the UWB channel parameters that can be met in a real scenario.

We focus on convex objects which can model humans in an UWB channel. These objects can be cylinders with R in the range $0.2 \le R \le 0.3$ [m] - compare [2]. The remaining parameters whose ranges must be found are frequency f, $\cos(\theta^i)$ and θ. We assume that $0.5 \le f \le 10$ [GHz] (typical UWB spectrum), $0.5\cdot10^{-3} \le \cos(\theta^i) \le 1$ and $0.5\cdot10^{-3} \le \theta \le 1.5\pi$ [rad].

With the above assumed bounds for UWB channel scenario parameters the limits of approximation variables are as follows: $10^{-11} \le -\xi^i_{sub} \le 10^2$, $10^{-11} \le \xi^d_{sub} \le 10^4$ (log scale sampling of approximation domains is used).

After performing VF approximations of $V^i\left(\xi^i_{sub}\right)$ and $V^d\left(\xi^d_{sub}\right)$ with the maximum 1% allowed error of approximation in the predefined domains limits we obtained 40 and 28 components approximating $V^i\left(\xi^i_{sub}\right)$ and $V^d\left(\xi^d_{sub}\right)$, respectively. Then, when we use (7a), (7b) as new variables, we can present the approximated forms of (6a) and (6b) by (8a) and (8b), respectively.

$$\xi^{wi} = \frac{\xi^{i}_{sub}}{\omega} \tag{7a}$$

$$\xi^{wd} = \frac{\xi^{d}_{sub}}{\omega} \tag{7b}$$

$$H^{i}_{rad}(\omega) \approx \sqrt{\frac{1}{4\pi R \cdot \cos^{3}(\theta^{i})}} \cdot \sum_{k=1}^{K^{i}=40} \frac{C^{i}_{k}\left(\xi^{wd}\right)^{-1}}{j\omega + A^{i}_{k}\left(\xi^{wd}\right)^{-1}} \tag{8a}$$

$$H^{d}_{rad}(\omega) \approx \sqrt{\frac{1}{4\pi R \cdot \theta^{3}}} \cdot \sum_{k=1}^{K^{d}=28} \frac{C^{d}_{k}\left(\xi^{wd}\right)^{-1}}{j\omega + A^{d}_{k}\left(\xi^{wd}\right)^{-1}} \tag{8b}$$

The corresponding time-domain equivalents of (8a) and (8b) are the sums of exponential functions, which can be easily found by applying the inverse Laplace transform to (8a-b).

We obtained the values of poles and residues, which are given in Tables I – IV. The poles and residues of VF approximation can be real as well as complex numbers. Our poles and residues are real numbers. The approximations (8a) and (8b) are valid when the following inequalities are fulfilled (f_L and f_H are the lower and upper limits of the considered frequency band of a time-domain derivative of a current source):

$$\frac{10^{-11}}{2\pi \cdot f_L} \leq \xi^{wi} \leq \frac{10^{2}}{2\pi \cdot f_H} \tag{9a}$$

$$\frac{10^{-11}}{2\pi \cdot f_L} \leq \xi^{wd} \leq \frac{10^{4}}{2\pi \cdot f_H} \tag{9b}$$

We set values of f_L and $f_{H,}$ as these frequencies for which the amplitude of input signal in frequency domain decreases to 2% of its maximum value.

TABLE I. POLES VALUES USED IN (8A)

A^{i}_{1}	-2.185543304217194e+003	A^{i}_{2}	-4.301968876076460e+002
A^{i}_{3}	-9.611494939819919e+001	A^{i}_{4}	-3.772272211339679e+001
A^{i}_{5}	-1.628376864828188e+001	A^{i}_{6}	-7.182617240778624e+000
A^{i}_{7}	-3.189549021407840e+000	A^{i}_{8}	-1.413201254180459e+000
A^{i}_{9}	-6.230434965339632e-001	A^{i}_{10}	-2.736555872357704e-001
A^{i}_{11}	-1.199612871557221e-001	A^{i}_{12}	-5.255002059714047e-002
A^{i}_{13}	-2.301979887397455e-002	A^{i}_{14}	-1.008723915116767e-002
A^{i}_{15}	-4.422253922239161e-003	A^{i}_{16}	-1.939678540271621e-003
A^{i}_{17}	-8.511853812932363e-004	A^{i}_{18}	-3.736907494332198e-004
A^{i}_{19}	-1.641262314699220e-004	A^{i}_{20}	-7.211172780755891e-005
A^{i}_{21}	-3.169444977566691e-005	A^{i}_{22}	-1.393477197099581e-005
A^{i}_{23}	-6.128420874688177e-006	A^{i}_{24}	-2.696030883584822e-006
A^{i}_{25}	-1.186388601593053e-006	A^{i}_{26}	-5.222230717642428e-007
A^{i}_{27}	-2.299410617616871e-007	A^{i}_{28}	-1.012783502874818e-007
A^{i}_{29}	-4.462407702632884e-008	A^{i}_{30}	-1.966950011122220e-008
A^{i}_{31}	-8.673919619800505e-009	A^{i}_{32}	-3.827115518857851e-009
A^{i}_{33}	-1.689696622739224e-009	A^{i}_{34}	-7.465866790530961e-010
A^{i}_{35}	-3.301521858258436e-010	A^{i}_{36}	-1.460673093134953e-010
A^{i}_{37}	-6.448971279707296e-011	A^{i}_{38}	-2.804416673506481e-011
A^{i}_{39}	-1.126184284210101e-011	A^{i}_{40}	-2.980982304356931e-012

TABLE II. RESIDUES VALUES USED IN (8A)

C^{i}_{1}	-1.820682236408822e+005	C^{i}_{2}	3.071231724127923e+004
C^{i}_{3}	8.353629163603452e+001	C^{i}_{4}	2.049331599578998e+002
C^{i}_{5}	2.139801080278334e+001	C^{i}_{6}	1.311357316555620e+001
C^{i}_{7}	2.530061595098228e+000	C^{i}_{8}	9.511185739238481e-001
C^{i}_{9}	2.162872803803492e-001	C^{i}_{10}	6.748436681283289e-002
C^{i}_{11}	1.712561896274437e-002	C^{i}_{12}	5.061354156339383e-003
C^{i}_{13}	1.373510685907707e-003	C^{i}_{14}	3.997999356334482e-004
C^{i}_{15}	1.123454516016146e-004	C^{i}_{16}	3.259514101474947e-005
C^{i}_{17}	9.322384641643496e-006	C^{i}_{18}	2.705915238839442e-006
C^{i}_{19}	7.810156972530819e-007	C^{i}_{20}	2.270100629010955e-007
C^{i}_{21}	6.584968985708626e-008	C^{i}_{22}	1.916749817973067e-008
C^{i}_{23}	5.576224664097102e-009	C^{i}_{24}	1.625219834766921e-009
C^{i}_{25}	4.737033251305995e-010	C^{i}_{26}	1.382212501093350e-010
C^{i}_{27}	4.034368083143569e-011	C^{i}_{28}	1.178452606379634e-011
C^{i}_{29}	3.443836502537814e-012	C^{i}_{30}	1.007097481177157e-012
C^{i}_{31}	2.946849076792510e-013	C^{i}_{32}	8.629375640339669e-014
C^{i}_{33}	2.529070772352165e-014	C^{i}_{34}	7.419927071527440e-015
C^{i}_{35}	2.179732553179911e-015	C^{i}_{36}	6.415258614102569e-016
C^{i}_{37}	1.894392881351826e-016	C^{i}_{38}	5.641285152532327e-017
C^{i}_{39}	1.706889806400305e-017	C^{i}_{40}	4.349974364231435e-018

TABLE III. POLES VALUES USED IN (8B)

A^{d}_{1}	-7.624938133543778e+004	A^{d}_{2}	-3.066554884403939e+004
A^{d}_{3}	-5.883627095728042e+003	A^{d}_{4}	-2.643835168169282e+003
A^{d}_{5}	-1.278501793762674e+003	A^{d}_{6}	-3.480483992918555e+002
A^{d}_{7}	-5.815674350458664e+001	A^{d}_{8}	-1.894761830271030e+001
A^{d}_{9}	-1.634895714365327e+000	A^{d}_{10}	-4.735134595242392e-001
A^{d}_{11}	-1.309616447852327e-001	A^{d}_{12}	-3.467873642750247e-002
A^{d}_{13}	-8.939641862286355e-003	A^{d}_{14}	-2.270789022037268e-003
A^{d}_{15}	-5.723416880966668e-004	A^{d}_{16}	-1.437023109881982e-004
A^{d}_{17}	-3.602368776444139e-005	A^{d}_{18}	-9.028417724844789e-006
A^{d}_{19}	-2.264062185478928e-006	A^{d}_{20}	-5.683885250794306e-007
A^{d}_{21}	-1.429050795391364e-007	A^{d}_{22}	-3.599547403013408e-008
A^{d}_{23}	-9.087230873873224e-009	A^{d}_{24}	-2.300739714481921e-009
A^{d}_{25}	-5.847087941863093e-010	A^{d}_{26}	-1.492114297297116e-010
A^{d}_{27}	-3.777889823532797e-011	A^{d}_{28}	-7.922667771832249e-012

TABLE IV. RESIDUES VALUES USED IN (8B)

C^{d}_{1}	-1.091354219751651e+002	C^{d}_{2}	4.893340038413864e+001
C^{d}_{3}	-7.177498779156004e+000	C^{d}_{4}	2.707387979612206e+001
C^{d}_{5}	-5.639975079688894e+001	C^{d}_{6}	8.050507641947452e+001
C^{d}_{7}	-3.590894225399839e+001	C^{d}_{8}	-1.055369311054441e+001
C^{d}_{9}	4.985092336329905e-001	C^{d}_{10}	1.323265777979574e-001
C^{d}_{11}	2.357458738517980e-002	C^{d}_{12}	3.538621423149182e-003
C^{d}_{13}	4.862875966584310e-004	C^{d}_{14}	6.405033723402427e-005
C^{d}_{15}	8.238383991771843e-006	C^{d}_{16}	1.046750900320124e-006
C^{d}_{17}	1.321157518849667e-007	C^{d}_{18}	1.662720586727687e-008
C^{d}_{19}	2.090914726905126e-009	C^{d}_{20}	2.631003375504038e-010
C^{d}_{21}	3.315544744011198e-011	C^{d}_{22}	4.187355252828445e-012
C^{d}_{23}	5.303425477752148e-013	C^{d}_{24}	6.741574703140609e-014
C^{d}_{25}	8.611517240098348e-015	C^{d}_{26}	1.107849814051965e-015
C^{d}_{27}	1.446018427494702e-016	C^{d}_{28}	1.935482892684701e-017

IV. MODELING OF SIMULATION IN SPICE

As a result of the approximation, described in the previous section, we obtain two transfer functions: $H_{rad}^{i}(s)$ and $H_{rad}^{d}(s)$ ($j\omega = s$), as a finite series of partial fractions. They can have the form of a single fraction, or a couple of complex conjugate fractions, which represents a partial transfer function of the two-ports, which are next used to build the subcircuits corresponding to each partial transfer function. The transfer function of the two possible two-ports has one of the following forms:

$$H_{1(k)}(s) = \frac{R_k}{s+p_k},$$
$$H_{2(k)}(s) = \frac{R_k}{s+p_k} + \frac{R_k^{*}}{s+p_k^{*}} = \frac{b_{1k}s + b_{0k}}{s^2 + a_{1k}s + a_{0k}}. \qquad (10)$$

The two-ports corresponding to transfer functions $H_{1(k)}(s)$, $H_{2(k)}(s)$ are shown in Fig. 2. a, b. The values of the circuit parameters are determined by the poles and the residues, which are fixed, and by the geometry of the radiation scenario.

Parameters R_k and p_k in (10) depend not only on residues and poles but also on geometrical parameters of a given obstacle (e.g. $C_k^i \cdot \xi^{wi^{-1}}$ and $p_k = A_k^i \cdot \xi^{wi^{-1}}$ in (8a)). Assuming that parameters R_k and p_k are known, we can calculate the value of circuit elements in Fig.2. a, b in the following way:

$$\mathrm{C} = \mathrm{C}_0 = 10\mathrm{pF},\quad \mathrm{R}_k = \frac{1}{\mathrm{C}_0 \mathrm{p}_k},\qquad \mathrm{h}_k = \frac{\mathrm{R}_k}{\mathrm{p}_k} \qquad \text{a)} \qquad (11)$$

$$\mathrm{R}_{2k}\mathrm{C}_1 = 1,\ \mathrm{h}_k = \mathrm{b}_{1k},\ \frac{\mathrm{h}_k}{\mathrm{C}_2} = \mathrm{b}_{0k},$$
$$\frac{\mathrm{R}_{2k}}{\mathrm{R}_{1k}} + \frac{\mathrm{C}_2}{\mathrm{C}_1} = \mathrm{a}_{1k},\ \frac{1}{\mathrm{R}_{1k}\mathrm{C}_2} + 1 - \mathrm{h}_k = \mathrm{a}_{0k}. \qquad \text{b)} \qquad (12)$$

We choose arbitrarily C_0 = 10pF. To obtain a circuit equivalent to each radiation ray we need also to connect an adder, an amplifier, corresponding to spreading factor A^C and a transmission line, corresponding to delay expression $exp\left(-s \cdot \frac{s^p}{V_0}\right)$, (1).

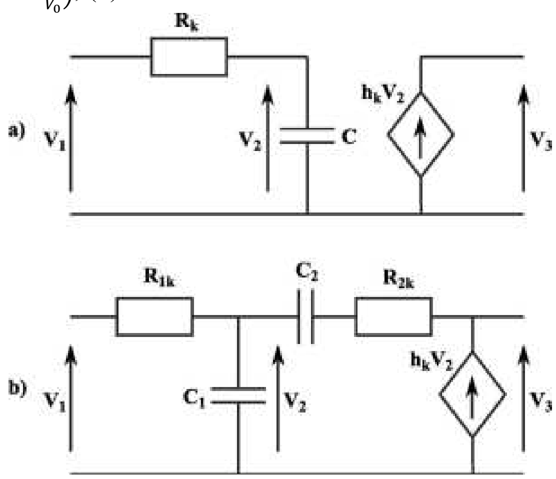

Fig. 2. Two-ports corresponding to: $H_{1(k)}(s)$-a), $H_{2(k)}(s)$-b).

V. NUMERICAL EXAMPLES

In this section we verify the results presented in Sections III and IV through simulations of radiation of EM wave from TE polarized magnetic current UWB sources placed on convex conducting 2D cylinder. The Spice simulation results are compared with IFFT results calculated with (1). We present two numerical examples. In the first the observation point is in the lit zone, while in the second the observation point is in the shadow zone. As a derivative of a magnetic current source (inverse Fourier transform of M(ω) in (1)) we use an UWB pulse given by (13) with t_c=1ns and a=0.2ns:

$$m(t) = \left[1 - 4\pi\left(\frac{t-t_c}{a}\right)^2\right] \times \exp\left[-2\pi\left(\frac{t-t_c}{a}\right)^2\right] \qquad (13)$$

The radius of the cylinder for both scenarios is 0.25m. The position of source (Q' in Fig. 1) is $\varphi_s=\pi/2$. The position of observation points for the first and second example are $\varphi_i=\pi/4$ and $\varphi_d=7\pi/4$, respectively with ρ=1.5m. The simulation results of the first example are shown in Figs 3, 4, 5, while the calculation results for the second example are shown in Figs 6, 7. The delay is not taken into account in the results. The maxima of the waveforms are normalized by the maximum of direct waveform. In the figures, for the purpose of space saving, only the results of x-component of an electric field are presented. The values of frequencies f_L and f_H are 0.32 GHz and 10.40 GHz, respectively. In the figures, the dotted line waveforms are calculated by IFFT, while the square mark waveforms are calculated directly in the time domain.

In all examples we can see that IFFT and SPICE simulation results are in very good agreement. The ranges of ξ_{sub}^{i} and ξ_{sub}^{d} for given ray scenarios fit in the limits given in Section III.

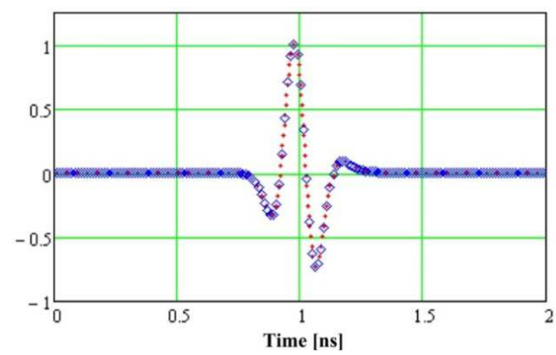

Fig. 3. The simulation results of the x-component of electric field radiated along the direct ray in example 1.

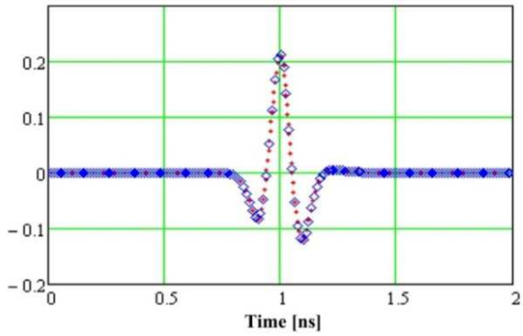

Fig. 4. The simulation results of the x-component of electric field radiated through shedding point Q1 example 1.

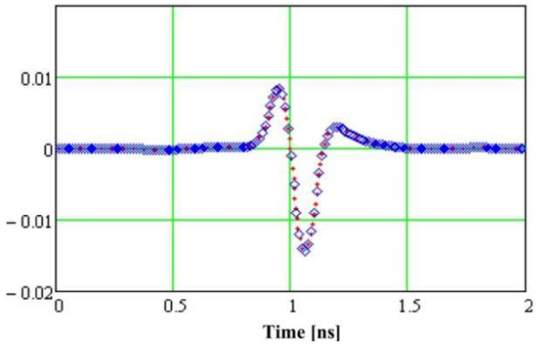

Fig. 5. The simulation results of the x-component of electric field radiated through shedding point Q2 example 1.

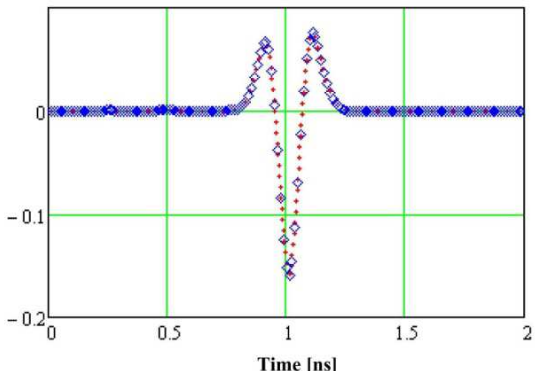

Fig. 6. The simulation results of the x-component of electric field radiated through shedding point Q1 example 2.

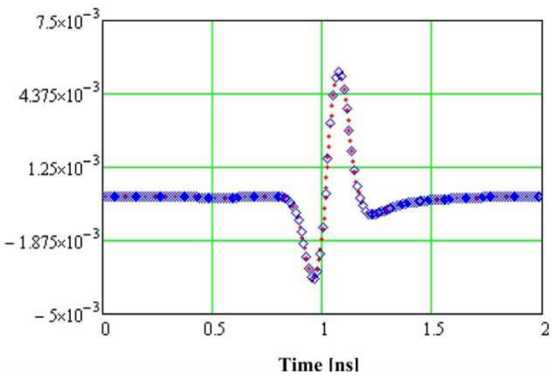

Fig. 7. The simulation results of the x-component of electric field radiated through shedding point Q2 example 1.

VI. CONCLUSIONS

In the paper we presented a universal rational approximation of the transfer function of the radiation ray for the case of radiation of EM wave by UWB sources placed on convex obstacle. The approximation is performed using the vector fitting algorithm, which is independent of the geometry of radiation scenario and the frequency band (of course within reasonable limits). In order to obtain the universal vector fitting approximation we introduced the new variables. We specified the ranges of these new variables (VF approximation domain limits) that reflect the practical values of the UWB channel parameters. The new approximated transfer functions have the form of a finite series of partial fractions. All the poles and residues of the transfer functions for the case of TE polarized magnetic current source are given in the paper. Various considered scenarios of radiation and various frequency bands can be modeled by using given poles and residues by controlling only the geometrical parameters of the scenarios (R, θ etc.).

The presented impulse response of a creeping ray has a very simple form, given by a sum of exponential functions. Therefore the obtained results are suitable for modeling radiation and propagation of EM wave in UWB channel containing convex obstacles in SPICE-like simulators. The great advantage of modeling in SPICE is the possibility of including detailed models of transmitter and receiver that consider their nonlinearities. Moreover in simulations of EM wave propagation we can implement very fast and effective convolution algorithms with any input signal [7].

REFERENCES

[1] M.Z. Win D. Porcino, W. Hirt , “Ultra-wideband radio technology: potential and challenges ahead”, *IEEE Communications Magazine*, July 2003, pp. 2-11,

[2] M. Ghaddar, L. Talbi, T. A. Denidni, A. Sebak, “A Conducting Cylinder for Modeling Human Body Presence in Indoor Propagation channel”, *IEEE Transactions on Antennas and Propagation*, vol. 55, no. 11, November 2007, pp. 3099-3103

[3] Hsi-Tseng Chou, P. H. Pathak, P. R. Rousseau, “TD-UTD Solutions for the Transient Radiation of Pulsed Antennas Placed on PEC smooth Convex Surfaces”, *IEEE Transactions on Antennas and Propagation*, vol. 59, no. 5, May 2011, pp. 1626-1637,

[4] P. H. Pathak, R. G. Kouyoumjian, “The radiation from Apertures in Curved Surfaces”, N*ational Aeronautics and Space Administration*, Washington, D. D, July 1973.

[4] B. Chaudhury, P.K. Chattopadhyay, D. Raju, S. Chaturvedi, “Transient Analysis of Creeping Wave Modes Using 3-D FDTD Simulation and SVD Method”, *IEEE Transactions on Antennas and Propagation*, vol. 57, no. 3, March 2009, pp. 754-759

[5] B. Gustavsen, A. Semlyen, “Rational approximation of frequency domain response by vector fitting”, *IEEE Transactions on Power Delivery*, vol.14, no. 3, 1999, pp. 1052-1061.

[6] D. A. McNamara, *Introduction to the uniform geometrical theory of diffraction*, Artech House, Boston, London, 1990.

[7] W. Janke, G. Blakiewicz, “Semi Analytical Recursive Algorithms for Convolution Calculations”, in *Proc. IEE - Circuits, Devices and Systems*, vol. 142, no. 2, April 1995, pp. 125-130